nature biotechnology

LETTERS

Increasing the efficiency of homology-directed repair for CRISPR-Cas9-induced precise gene editing in mammalian cells

Van Trung Chu[1], Timm Weber[1], Benedikt Wefers[2,3], Wolfgang Wurst[2–4], Sandrine Sander[1], Klaus Rajewsky[1] & Ralf Kühn[1,2,5]

© 2015 Nature America, Inc. All rights reserved.

The insertion of precise genetic modifications by genome editing tools such as CRISPR-Cas9 is limited by the relatively low efficiency of homology-directed repair (HDR) compared with the higher efficiency of the nonhomologous end-joining (NHEJ) pathway. To enhance HDR, enabling the insertion of precise genetic modifications, we suppressed the NHEJ key molecules KU70, KU80 or DNA ligase IV by gene silencing, the ligase IV inhibitor SCR7 or the coexpression of adenovirus 4 E1B55K and E4orf6 proteins in a 'traffic light' and other reporter systems. Suppression of KU70 and DNA ligase IV promotes the efficiency of HDR 4–5-fold. When co-expressed with the Cas9 system, E1B55K and E4orf6 improved the efficiency of HDR up to eightfold and essentially abolished NHEJ activity in both human and mouse cell lines. Our findings provide useful tools to improve the frequency of precise gene modifications in mammalian cells.

The CRISPR-Cas9 systems (clustered, regularly interspaced, short palindromic repeats (CRISPR)–CRISPR-associated protein) represent a versatile tool for genome engineering, enabling the induction of site-specific genomic double-strand breaks (DSBs) by single guide RNAs (sgRNAs)[1]. In mammalian cells DSBs are mostly repaired by the nonhomologous end-joining (NHEJ) pathway[2,3], frequently leading to the loss of nucleotides from the ends of DSBs. This enables the efficient construction of knockout alleles through the induction of frameshift mutations[4]. By contrast, the alternative pathway of homology-directed repair (HDR) can be used for the introduction of precise genetic modifications such as codon replacements or reporter insertions by recombination with exogenous targeting vectors, serving as repair template[5]. We reasoned that the efficiency of HDR and thus the construction of precise genetic modifications could be boosted by the transient inhibition of NHEJ key molecules, similar to what has been observed for *Drosophila* embryos with a genetic DNA ligase IV deficiency[6].

To quantitatively determine the outcome of CRISPR-Cas-induced DSB repair, we first generated human HEK293 cells with a 'traffic light' reporter[7] (TLR) vector integrated into the adeno-associated virus integration site 1 (AAVS1) locus[8] (**Fig. 1a**). HEK293 cells were transfected with an AAVS1 targeting vector carrying the TLR insert and expression plasmids for Cas9 and an AAVS1-specific sgRNA (**Supplementary Fig. 1**). Upon selection and genotyping of transfected cells, we obtained heterozygous ($AAVS1^{TLR/+}$) and homozygous ($AAVS1^{TLR/TLR}$) targeted clones harboring the TLR construct in the AAVS1 locus (**Supplementary Fig. 2**). The reporter includes a CAG promoter for expression of a nonfunctional green fluorescent (Venus) gene, disrupted by the replacement of codons 117–152 with target sequences from the mouse *Rosa26* and *Rab38* locus, followed by coding regions for a self-cleaving 2A peptide and a red fluorescent (TagRFP) gene in a reading frame shifted by 2 bp (**Supplementary Table 1**). CRISPR-Cas9-induced DSBs in the target region that are repaired by means of NHEJ and cause deletions shift the translation to the frame of the 2A-TagRFP in about 1/3 of the mutagenic NHEJ events; this can be detected in reporter cells by the expression of RFP (**Fig. 1b**). If an intact Venus coding region is provided as repair template, cells that repair the DSBs by HDR express Venus. For activation of the TLR reporter, we designed two sgRNAs against the *Rosa26* target sequence, of which sgRosa26-1 showed a higher activity to induce deletions in the endogenous locus of mouse NIH3T3 cells (**Fig. 1c**).

Next, we transfected $AAVS1^{TLR/+}$ cells with an expression vector for Cas9, blue fluorescent protein (BFP) and sgRosa26-1, together with a linearized Venus donor plasmid. 72 h after transfection the cells were analyzed by FACS, gated for BFP^+ transfected cells, and the frequency of $Venus^+$ and of RFP^+ cells was determined. We observed 3% RFP^+ and 5% $Venus^+$ cells, indications of NHEJ or HDR repair events, respectively, as compared to 0.1% RFP^+ and 0.6% $Venus^+$ cells in a control lacking sgRosa26-1 (**Fig. 1d**). Of note, RFP^+ cells detected by the TLR assay represent only 1/3 of all mutagenic NHEJ events. Similar results were obtained with $AAVS1^{TLR/TLR}$ cells (**Supplementary Fig. 3**).

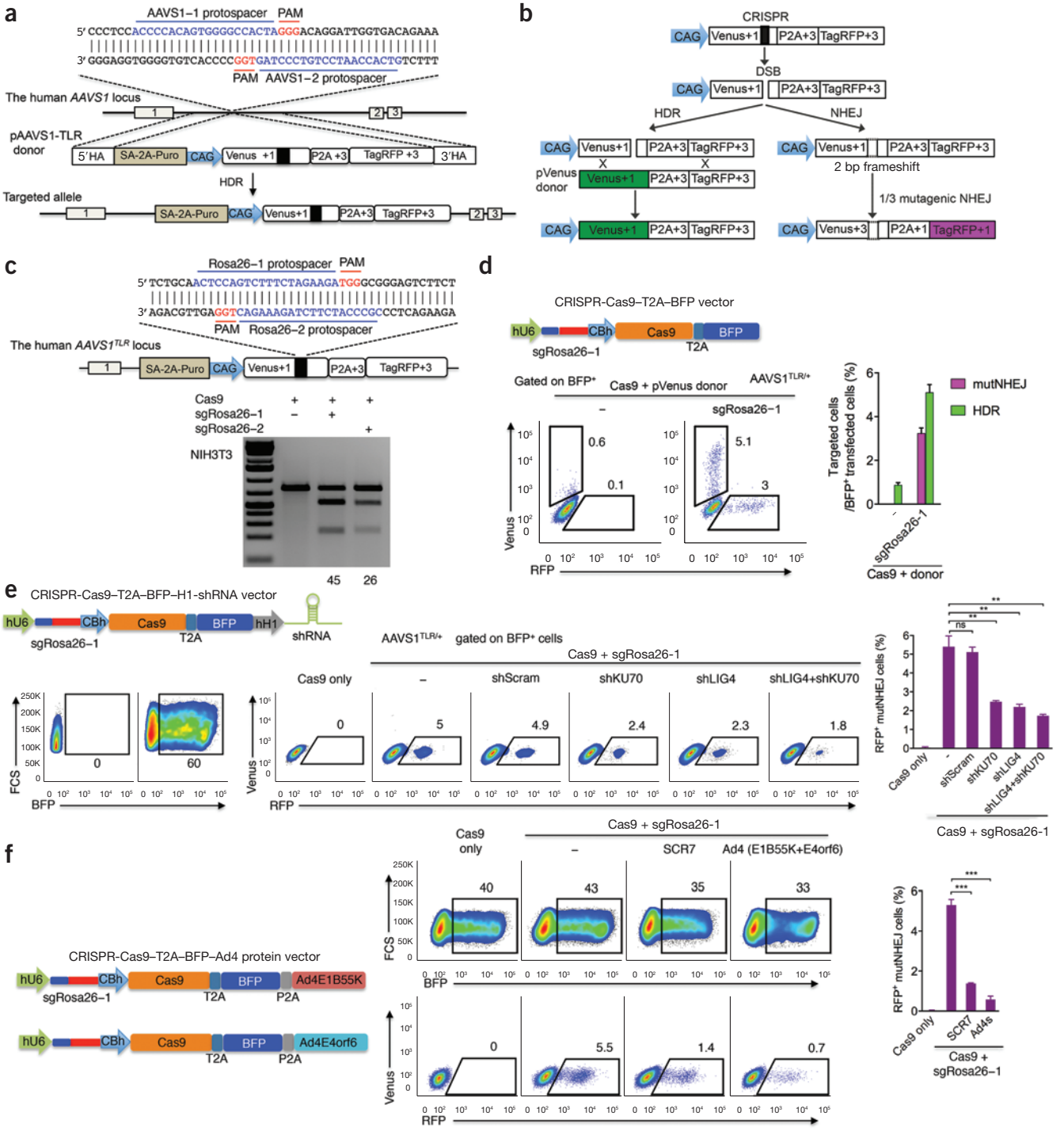
For suppression of key NHEJ pathway proteins[2,9] by short hairpin (sh) RNAs, we added a human H1 promoter to the sgRosa26-1/Cas9/BFP expression vector and inserted published shRNA sequences to knock down KU70, KU80 or DNA ligase IV. We first determined the extent of NHEJ suppression by transfection of $AAVS1^{TLR/+}$ cells with different

[1]Max-Delbrück-Center for Molecular Medicine, Berlin, Germany. [2]Helmholtz Zentrum München, German Research Center for Environmental Health, Neuherberg, Germany. [3]Deutsches Zentrum für Neurodegenerative Erkrankungen e.V., Munich, Germany. [4]Munich Cluster for Systems Neurology (SyNergy), Ludwig-Maximilians-Universität München, Munich, Germany. [5]Berlin Institute of Health, Berlin, Germany. Correspondence should be addressed to R.K. (ralf.kuehn@mdc-berlin.de) or K.R. (klaus.rajewsky@mdc-berlin.de).

Received 13 February; accepted 18 March; published online 24 March 2015; doi:10.1038/nbt.3198

sgRosa26-1–Cas9-BFP-H1 shRNA expression vectors in the absence of a repair template. 72 h after transfection the samples were analyzed for RFP$^+$ cells and compared to controls that had either a scrambled shRNA or no shRNA. A substantial suppression of NHEJ repair was observed upon the individual or combined knockdown of KU70, KU80 or DNA ligase IV (**Fig. 1e** and **Supplementary Fig. 4**). Similar results were obtained in AAVS1$^{TLR/TLR}$ cell lines by the knockdown of KU70, KU80 or DNA ligase IV (**Supplementary Fig. 4**). The knockdown of ligase IV reduced its protein level in transfected AAVS1^{TLR} (BFP$^+$) cells by 70% (**Supplementary Fig. 5**).

As additional approaches to DNA ligase IV inhibition, we used the small-molecule inhibitor SCR7 (ref. 10) or the adenovirus 4 (Ad4) E1B55K and E4orf6 proteins, which mediate the ubiquitination and proteasomal degradation of DNA ligase IV[11,12]. For the coexpression of Ad4 proteins, sgRosa26-1, Cas9 and BFP from a vector pair, we linked the Ad4 E1B55K or the Ad4 E4orf6 gene by self-cleaving 2A peptide sequences to BFP (**Fig. 1f**). Mono- or biallelic AAVS1^{TLR} cell lines were transfected with either the sgRosa26-1–Cas9-BFP expression vector (in the presence or absence of SCR7 inhibitor) or both sgRosa26-1/Cas9/BFP/Ad4 E1B55K and E4orf6 plasmids. The presence of SCR7



© 2015 Nature America, Inc. All rights reserved.

reduced the fraction of RFP$^+$ cells in the BFP$^+$ population fourfold whereas the coexpression of Ad4 proteins led to an eightfold reduction, compared to controls lacking inhibitor or Ad4 proteins (**Fig. 1f** and **Supplementary Fig. 6**). The coexpression of Ad4 proteins reduced the level of DNA ligase IV protein in transfected AAVS1^{TLR} (BFP$^+$) cells by 93% (**Supplementary Fig. 5**). Overall, these results show that the NHEJ repair of CRISPR-Cas9-induced DSBs can be suppressed by targeting DNA ligase IV using RNA interference, SCR7 or, most efficiently, the Ad4 proteins.

To assess the effect of NHEJ suppression on HDR, we transfected AAVS1$^{TLR/+}$ cells with Venus repair template together with sgRosa26-1/Cas9/BFP vector (with and without SCR7) or with sgRosa26-1/Cas9/BFP vectors including either the Ad4 proteins or shRNA constructs targeting KU70, KU80 or DNA ligase IV. After 72 h the frequency of RFP$^+$ and Venus$^+$ cells within BFP$^+$ cells was analyzed by FACS (**Fig. 2a**,**b** and **Supplementary Fig. 7**). Venus$^+$ (HDR) cells increased from 5% for sgRosa26-1/Cas9/BFP alone, to 8–14% in the presence of single shRNAs against KU70, KU80 or DNA ligase IV, to 25% in the presence of shRNAs against KU70 and DNA ligase IV or 1 μM of the inhibitor SCR7, and further to 36% upon the coexpression of the Ad4 proteins. Thus, HDR efficiency was enhanced up to fivefold in the presence of KU70 and ligase IV shRNAs or SCR7, and up to sevenfold by the Ad4 protein pair (**Fig. 2c** and **Supplementary Fig. 8**).

Titration of SCR7 on AAVS1$^{TLR/+}$ cells showed an optimal effect at 1 μM concentration (**Supplementary Fig. 9**). For cells in the presence of two shRNAs, SCR7 or Ad4 proteins, we noticed diminished fluorescence signals within the population of Venus$^+$ cells at 72 h after transfection (**Fig. 2a** and **Supplementary Figs. 7**,**9c**), indicating reduced Venus expression in cells undergoing NHEJ blockade, possibly caused by local chromatin remodeling through an extended DNA damage response[13,14]. However, Venus expression was normal in clones established from AAVS1$^{TLR/+}$ cells targeted in the presence of Ad4 proteins, indicating that this effect is only transient (**Supplementary Fig. 9d**). From the sample expressing the Ad4 proteins, Venus$^+$ cells were sorted, and we established 24 clones to confirm the integrity of the repaired TLR loci using PCR and sequence analysis (**Supplementary Table 2**). In contrast to the increase of Venus$^+$ cells, RFP$^+$ cells decreased from 3% in the controls to 1.7%, 1.4% or 0.6% in the presence of shRNAs, SCR7 or Ad4 proteins, respectively (**Fig. 2a**,**b**). Whether the residual NHEJ activity relies on the KU- and ligase IV–independent alternative end-joining mechanism[15] remains to be determined.

Assessing the influence of the lengths of homology regions of the repair template on HDR efficiency, we generated donor templates with 3′ homology regions shortened from 1,450 bp as in the original donor template to 350 bp (**Fig. 2d** and **Supplementary Fig. 10**). We transfected AAVS1$^{TLR/+}$ cells with sgRosa26-1/Cas9/BFP expression vector and each of the various donor templates, with or without the coexpression of Ad4 proteins. FACS analysis revealed a reduced targeting frequency (2%) for the donor with a 350 bp 3′ homology region whereas the other molecules showed HDR efficiencies in the range of 5% (**Fig. 2e**). In the presence of Ad4 proteins the frequency of Venus$^+$ cells increased robustly up to 25% for the 350-bp donor and to 30% for the other donor molecules. In line with the previous results, the frequency of RFP$^+$ cells was strongly reduced by the coexpression of Ad4 proteins (**Fig. 2f**). Thus, PCR-generated fragments with combined homology regions of >1 kb are effective donors for HDR (**Fig. 2e**,**f** and **Supplementary Fig. 10**).

Applying our approach to an endogenous genomic locus, we inserted a GFP reporter gene into the *AAVS1* locus of HEK293 cells. The AAVS1-SA-T2A-GFP targeting vector includes AAVS1 homology regions flanking a splice acceptor site and a 2A peptide sequence linked to GFP, enabling reporter expression by the AAVS1-derived transcript (**Fig. 2g**). HEK293 cells were cotransfected with an AAVS1-specific sgRNA/Cas9/mCherry (AAVS1-1/Cas9/mCherry) expression plasmid and the AAVS1-SA-T2A-GFP targeting vector, with or without coexpression of Ad4 proteins. 72 h after transfection the mCherry$^+$ transfected population exhibited 8% GFP$^+$ cells upon expression of sgAAVS1-1/Cas9 alone whereas the coexpression of Ad4 proteins raised the frequency of the cells to 66% (**Fig. 2h**). Thus, in line with the TLR results, we observed an eightfold stimulation of gene targeting at the *AAVS1* locus by the coexpression of Ad4 proteins. FACS sorting and cloning GFP$^+$ cells 48 h after transfection, we found correct GFP gene integration in 45 of 48 samples (95%), but only in 60% of the clones derived from the sample without Ad4 proteins (**Supplementary Fig. 11** and **Supplementary Table 3**), the remaining cells presumably representing random integrants.

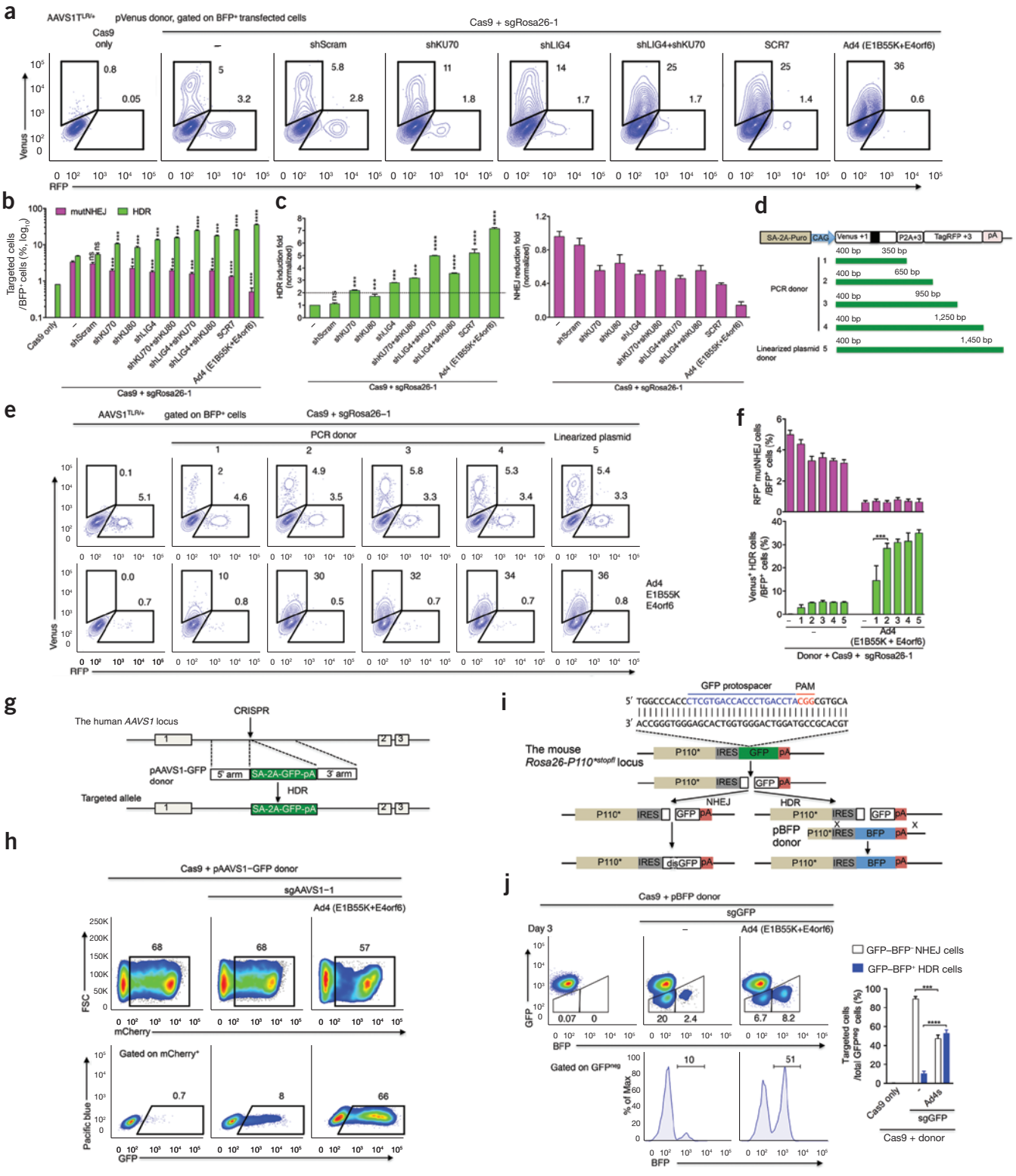
Coexpression of Ad4 proteins also promoted HDR efficiency in a mouse Burkitt lymphoma (BL) cell line containing an activated PI3 kinase α-subunit[16] linked to an IRES element and a GFP reporter in the *Rosa26* locus. We targeted the GFP using a specific sgRNA and a promoterless donor vector replacing GFP by BFP (**Fig. 2i**). The fraction of BFP$^+$ cells indicates HDR efficiency whereas the fraction of GFP$^-$ cells indicates

Figure 1 Insertion of a traffic light reporter into the *AAVS1* locus of HEK293 cells and suppression of the NHEJ pathway. (**a**) Strategy for insertion of the TLR construct into the *AAVS1* locus using CRISPR-Cas9 in human HEK293 cells. In the targeted sequence, the AAVS1-specific sgRNA is indicated in blue and the PAM signal is shown in red. The pAAVS1-TLR targeting vector includes homology arms (HA) of 800 bp flanking a splice acceptor (SA)-2A-puromycin element and the traffic light reporter insert comprising a CAG promoter and a Venus gene inactivated by the replacement of 36 codons with target sequences from the mouse Rosa26/Rab38 loci (black insert). (**b**) Diagram of the TLR system. CRISPR-Cas9-induced DSBs in the target region, repaired by NHEJ resulting in deletions that shift translation by 2 bp, led to RFP expression. An intact Venus coding region serves as repair template for HDR, leading to Venus expression. (**c**) Strategy to target the human *AAVS1^{TLR}* locus. Two different protospacers targeting the mouse *Rosa26-derived* sequence that interrupts the Venus gene are indicated in blue, with PAM signals in red. NIH3T3 cells were transfected by empty vectors or vectors expressing sgRosa26-1 or sgRosa26-2/Cas9-T2A-mCherry to test cutting efficiency in the endogenous *Rosa26* locus. 48 h after transfection, mCherry$^+$ cells were sorted and PCR and T7EI assays performed. The percentage of indels was quantified by the ImageJ software. (**d**) AAVS1^{TLR} cells were co-transfected with linearized Venus repair vector and Cas9-BFP expression plasmids with or without (–) sgRosa26-1. 72 h after transfection, flow cytometric analysis of BFP$^+$ gated cells displayed 5% of Venus$^+$ (HDR repair) cells and 3% of RFP$^+$ (NHEJ repair) cells. The graphs represent triplicate data from one of three independent experiments with similar results, shown as mean ± s.d. (**e**) Inhibition of the NHEJ pathway using gene silencing. Scheme of the sgRosa26-1/Cas9-2A-BFP-H1shRNA expression vector. AAVS1^{TLR} cells were transfected with sgRosa26-1/Cas9-2A-BFP (-) or sgRosa26-1/Cas9-2A-BFP-H1-shScrambled, -shKU70, -shLIG4 or -shKU70 or -shLIG4. 3 days later, these cells were analyzed by flow cytometry, gated on BFP$^+$ transfected cells, and the percentage of RFP$^+$ cells was determined. The graphs represent triplicate data from 1 of 3 independent experiments with similar results, shown as mean ± s.d. (**f**) Suppression of NHEJ repair using the ligase IV inhibitor SCR7 or the coexpression of ligase IV degrading Ad4 E1B55K and E4orf6 (Ad4s) proteins. AAVS1^{TLR} cells were transfected with sgRosa26-1/Cas9-2A-BFP expression vector (-) or transfected and cultured with SCR7 or were transfected with the sgRosa26-1/Cas9-2A-BFP-Ad4-E1B55K or -E4orf6 expression vectors. The samples were analyzed 3 days later by flow cytometry, gating on the BFP$^+$ transfected cells, and the percentage of RFP$^+$ cells was determined. The graphs represent triplicate data from one of six independent experiments with similar results, shown as mean ± s.d. Significance was calculated using the Student's *t*-test: $^{**}P < 0.01$, $^{***}P < 0.001$, ns, not significant.

© 2015 Nature America, Inc. All rights reserved.

NHEJ-mediated deletion events. Mouse BL cells were electroporated with Cas9 and the BFP replacement vector alone or with GFP-specific sgRNA/Cas9 expression plasmid with or without the coexpression of Ad4 proteins. Electroporation with sgGFP and Cas9 led to a transfection efficiency of 40%, as determined by mCherry expression after 24 h. About half of the transfected cells (22% in total) lost GFP expression after 72 h (**Supplementary Fig. 12**) and 10% of the GFP$^-$ cells were BFP$^+$ (**Fig. 2j**). The addition of Ad4 proteins reduced transfection efficiency to 27%, but again about half of the transfected cells (14% in total) lost GFP expression after 72 h (**Supplementary Fig. 12**). Notably, 50% of the GFP$^-$ cells were now BFP$^+$ (**Fig. 2j**), indicating a fivefold stimulation of HDR by Ad4 proteins.

To assess whether a point mutation can be corrected in a tumor cell line, we reverted the T24P codon replacement in the *Foxo1* gene



© 2015 Nature America, Inc. All rights reserved.

of mouse BL cells, which renders FOXO1 resistant to AKT-dependent phosphorylation. We transfected BL cells with a mutation-specific sgRNA and a second sgRNA recognizing the first intron, expression vectors for Cas9 and fluorescent reporters without or together with Ad4 proteins and a targeting vector containing the reverted codon 24 (and harboring a silent nucleotide replacement) and a puromycin-resistance gene (**Supplementary Fig. 13**). At day 2 transfected cells were isolated by FACS sorting, subjected to puromycin selection, and 53 or 39 clones derived from single cells were established from the sample without or with coexpression of Ad4 proteins, respectively. Genotyping of these clones by PCR and sequence analysis showed that 43 of the 53 clones derived without Ad4 proteins were mutants, 33 of these were heterozygous and 10 clones (19%) were targeted on both alleles. In the presence of Ad4 proteins, we found that all 39 clones were targeted, 24 of these were heterozygous and 15 clones (38%) homozygous mutants. Thus, despite the expected high targeting rate achieved with a selectable donor vector, the coexpression of Ad4 proteins further increased the targeting efficiency to 100% and doubled the net yield of homozygous, targeted clones.

In summary, we show that for CRISPR-Cas9-induced mutagenesis the suppression of the NHEJ key enzyme DNA ligase IV is an effective way for engineering precisely targeted mutations into the genome of mammalian cells. The activity of ligase IV can be blocked by gene silencing, small-molecule inhibition or proteolytic degradation, offering diverse approaches for the optimal delivery into target cells. For the proteolytic degradation of DNA ligase IV, we selected the E1B55K and E4orf6 proteins of adenovirus 4, shown to exert minimal influence on other cellular substrates such as Mre11 or p53, which are co-targeted by many other serotypes[17]. Nevertheless, we cannot exclude the possibility that HDR stimulation by the Ad4 proteins is mediated by the combined suppression of DNA ligase IV and other regulatory proteins. It could be of further interest to compare the effect on HDR of the E1B55K and E4orf6 proteins of additional adenoviral serotypes and species identified from humans[18] and other vertebrates[19]. Furthermore, the use of Ad4 proteins may be also beneficial for the construction of targeted mouse mutants, as recently shown for zygotes cultured in the presence of SCR7 (ref. 20). In populations of cells transfected with a sgRNA, Cas9 and Ad4 protein expression plasmids, we presently reach knock-in frequencies of 50–66%. By delivering Cas9 and sgRNAs as synthetic RNAs it may be possible, as shown for human induced pluripotent stemcells[21], to further enhance gene targeting efficiencies. It will be interesting to apply CRISPR-Cas9 mutagenesis combined with NHEJ suppression also to early embryos of other model organisms and to primary mammalian cells to achieve gene corrections.

Figure 2 Enhancement of HDR for CRISPR-Cas9-induced precise gene targeting. (**a**) Improvement of HDR efficiency by suppression of NHEJ key molecules. AAVS1^{TLR} cells were cotransfected with linearized Venus repair vector and sgRosa26-1/Cas9/BFP expression plasmid together with shRNA cassettes, SCR7 inhibitor or the Ad4 E1B55K/E4orf6 proteins. The frequency of RFP$^+$ and Venus$^+$ cells within the transfected BFP$^+$ population was determined by flow cytometry. The data represent one of four independent experiments with similar results. (**b**) The graph summarizes the frequency of RFP$^+$ (pink bars, significance compared to the (–) sample) and of Venus$^+$ (green bars; significance compared to the (–) sample) cells determined as in **a**. The *y* axis is represented as $\log_{10}$ scale. The bars represent mean values ± s.d. (**c**) Relative increase of HDR efficiency (significance compared to the (–) sample) and of NHEJ suppression normalized to the control transfected with sgRosa26-1/Cas9 and targeting vector alone (–). The dotted line indicates a more than twofold increase of HDR. The bars represent mean values ± s.d. (**d**) Use of PCR-generated donor templates. Scheme of the TLR construct and of PCR donor fragments, having a constant 5′ homology region of 400 bp whereas the length of the 3′ homology region varies from 350 bp to 1,250 bp; as control the linearized promoterless Venus repair vector was used. (**e**) AAVS1^{TLR} cells were cotransfected with sgRosa26-1/Cas9/BFP expression vector, the same molar amounts (800 fmol) of PCR donors or linearized Venus repair vector without or together with Ad4 E1B55K/E4orf6 proteins. The percentage of Venus$^+$ and RFP$^+$ cells was analyzed by flow cytometry 3 days after transfection. (**f**) The graph summarizes the frequency of RFP$^+$ (purple bars) and Venus$^+$ (green bars) cells determined as in **e**. The data represent one of two independent experiments with similar results. The bars represent mean values ± s.d. (**g**) Strategy for insertion of a GFP reporter gene into the human *AAVS1* locus using CRISPR-Cas9 in human HEK293 cells. The CRISPR-Cas9-targeted site is shown in **Figure 1a**; in the AAVS1-GFP targeting vector the GFP gene is flanked by AAVS1 homology regions of 800 bp. (**h**) HEK293 cells were cotransfected with linearized AAVS1-GFP targeting vector and with sgAAVS1-1/Cas9/mCherry expression vector or with sgAAVS1-1/Cas9/mCherry-Ad4-E1B55K and -E4orf6 expression vectors. At day 3, the frequency of GFP$^+$ cells within the population of mCherry+ transfected cells was analyzed using the flow cytometric data; shown is one of triplicate samples obtained from one of two independent experiments. (**i**) Fluorescent reporter replacement in the mouse BL cell line. The cell line harbors an activated PI3 kinase (P110*)-IRES-GFP-pA cassette in the *Rosa26* locus. In the targeted GFP sequence, the sgGFP target sequence is highlighted in blue and the PAM element in red. DSBs repaired by the NHEJ pathway led to the inactivation of GFP. DSBs repaired by HDR with the pBFP donor template led to the replacement of GFP by the BFP reporter gene. (**j**) Mouse BL cells were electroporated with Cas9/mCherry or sgGFP/Cas9/mCherry expression vector and the pBFP donor plasmid without or together with coexpression of the Ad4 E1B55K/E4orf6 proteins. The frequency of GFP$^-$BFP$^-$ (white bars) and GFP$^-$BFP$^+$ (blue bars) cells was analyzed at day 3. The graph summarizes triplicate results from one of three independent experiments with similar results. The bars represent mean values ± s.d. Significance was calculated using the Student's *t*-test: $^{**}P < 0.01$, $^{***}P < 0.001$, $^{****}P < 0.0001$, ns, not significant.

METHODS

Methods and any associated references are available in the online version of the paper.

Note: Any Supplementary Information and Source Data files are available in the online version of the paper.

ACKNOWLEDGMENTS

We thank K. Petsch and H.P. Rahn from the FACS core facility for excellent technical support. This work was supported by the European Research Council (ERC advanced grant ERC-AG-LS6, to K.R.), the German Ministry of Education and Research within the VIP program (TAL-CUT 03V0261, to W.W. and R.K.) and the European Union within the EUCOMMTOOLS project (FP7-HEALTH-F4-2010-261492, to W.W.). The plasmids MSCV-IRES-mCherry and MSCV-IRES-BFP were kind gifts of F. Rosenbauer and M. Janz (Charite, Berlin). We are grateful to H. Ploegh for communicating to us unpublished results and support in coordinating publication.

AUTHOR CONTRIBUTIONS

V.T.C., K.R. and R.K. conceived and designed the project, V.T.C. and T.W. acquired the data, V.T.C., K.R., T.W. and R.K. analyzed and interpreted the data, B.W., S.S. and W.W. provided materials, and V.T.C., K.R. and R.K. wrote the paper.

COMPETING FINANCIAL INTERESTS

The authors declare competing financial interests: details are available in the online version of the paper.

Reprints and permissions information is available online at http://www.nature.com/reprints/index.html.

1. Hsu, P.D., Lander, E.S. & Zhang, F. Development and applications of CRISPR-Cas9 for genome engineering. *Cell* **157**, 1262–1278 (2014).
2. Lieber, M.R. The mechanism of double-strand DNA break repair by the nonhomologous DNA end-joining pathway. *Annu. Rev. Biochem.* **79**, 181–211 (2010).
3. Mao, Z., Bozzella, M., Seluanov, A. & Gorbunova, V. Comparison of nonhomologous end joining and homologous recombination in human cells. *DNA Repair (Amst.)* **7**, 1765–1771 (2008).
4. Shalem, O. *et al.* Genome-scale CRISPR-Cas9 knockout screening in human cells. *Science* **343**, 84–87 (2014).
5. San Filippo, J., Sung, P. & Klein, H. Mechanism of eukaryotic homologous recombination. *Annu. Rev. Biochem.* **77**, 229–257 (2008).

© 2015 Nature America, Inc. All rights reserved.

6. Bozas, A., Beumer, K.J., Trautman, J.K. & Carroll, D. Genetic analysis of zinc-finger nuclease-induced gene targeting in *Drosophila*. *Genetics* **182**, 641–651 (2009).
7. Certo, M.T. *et al.* Tracking genome engineering outcome at individual DNA breakpoints. *Nat. Methods* **8**, 671–676 (2011).
8. Samulski, R.J. *et al.* Targeted integration of adeno-associated virus (AAV) into human chromosome 19. *EMBO J.* **10**, 3941–3950 (1991).
9. Panier, S. & Durocher, D. Push back to respond better: regulatory inhibition of the DNA double-strand break response. *Nat. Rev. Mol. Cell Biol.* **14**, 661–672 (2013).
10. Srivastava, M. *et al.* An inhibitor of nonhomologous end-joining abrogates double-strand break repair and impedes cancer progression. *Cell* **151**, 1474–1487 (2012).
11. Cheng, C.Y. *et al.* The E4orf6/E1B55K E3 ubiquitin ligase complexes of human adenoviruses exhibit heterogeneity in composition and substrate specificity. *J. Virol.* **85**, 765–775 (2011).
12. Forrester, N.A. *et al.* Serotype-specific inactivation of the cellular DNA damage response during adenovirus infection. *J. Virol.* **85**, 2201–2211 (2011).
13. Adam, S. & Polo, S.E. Blurring the line between the DNA damage response and transcription: the importance of chromatin dynamics. *Exp. Cell Res.* **329**, 148–153 (2014).
14. Zhu, Q. & Wani, A.A. Histone modifications: crucial elements for damage response and chromatin restoration. *J. Cell. Physiol.* **223**, 283–288 (2010).
15. Frit, P., Barboule, N., Yuan, Y., Gomez, D. & Calsou, P. Alternative end-joining pathway(s): bricolage at DNA breaks. *DNA Repair (Amst.)* **17**, 81–97 (2014).
16. Srinivasan, L. *et al.* PI3 kinase signals BCR-dependent mature B cell survival. *Cell* **139**, 573–586 (2009).
17. Cheng, C.Y. *et al.* The E4orf6/E1B55K E3 ubiquitin ligase complexes of human adenoviruses exhibit heterogeneity in composition and substrate specificity. *J. Virol.* **85**, 765–775 (2011).
18. Ghebremedhin, B. Human adenovirus: viral pathogen with increasing importance. *Eur. J. Microbiol. Immunol.* **4**, 26–33 (2014).
19. Benk , M. et al. in Virus Taxonomy, Eighth Report of the International Committee on Taxonomy of Viruses (Elsevier Academic Press, 2005).
20. Singh, P., Schimenti, J.C. & Bolcun-Filas, E. A mouse geneticist's practical guide to CRISPR applications. *Genetics* **199**, 1–15 (2015).
21. González, F. *et al.* An iCRISPR platform for rapid, multiplexable, and inducible genome editing in human pluripotent stem cells. *Cell Stem Cell* **15**, 215–226 (2014).

© 2015 Nature America, Inc. All rights reserved.

ONLINE METHODS

Traffic light reporter construct. The traffic light reporter (TLR) expression construct was assembled by cloning of PCR fragments encoding a defective Venus (codons 117–152 replaced by a 52-bp segment derived from the mouse *Rosa26* locus (sgRNA target sequence underlined) and a 56-bp segment from the mouse *Rab38* gene) linked to the 2A peptide from *Thosea asigna*[22] and the coding region of TagRFP[23] in a 2-bp shifted reading frame (+3), cloned in between the CAG promoter and the polyA region of the bovine hGH gene. The CAG promoter was deleted from this plasmid to derive the traffic light targeting vector (**Supplementary Table 1**).

Cell culture and reagents. Wild-type, AAVS1^{TLR} HEK293 and mouse NIH3T3 cells were maintained in DMEM (Gibco) supplied with 15% FBS (Gibco), cells were passaged three times per week. The mouse Burkitt lymphoma cell line, generated from a Burkitt-like mouse lymphoma[16] was maintained in DMEM supplied with 15% FBS, 2 mM HEPES (Gibco), 2 mM sodium pyruvate (Gibco), 2 mM L-glutamine (Gibco), and 1× NAA (Gibco), beta-mercaptoethanol (Sigma) and passaged four times per week. For puromycin selection, mCherry$^+$ cells were sorted, seeded at 10^3 cells/well and selected with 3 μg/ml of Puromycin for 2 weeks. Then colonies were counted and single cells were sorted. The SCR7 inhibitor was purchased (Xcess Biosciences, San Diego, USA), 12 h after transfection these cells were maintained in complete medium supplied with 1 μM SCR7 inhibitor until analysis. At SCR7 concentrations of 60 μM and 10 μM, we observed a reduction of transfection efficiency and of cell viability.

Donor vectors and CRISPR-Cas9-T2A-reporter vectors. To generate the CRISPR-Cas9-T2A reporter vector, we amplified T2A-mCherry and T2A-BFP fragment by overlapping PCR and cloned them into FseI/EcoRI sites of plasmid pX330 (Addgene, #42230). The mCherry and BFP templates were derived from the plasmids MSCV-IRES-mCherry and MSCV-IRES-BFP, respectively, a kind gift of Frank Rosenbauer and Martin Janz (Charite, Berlin). To generate the AAVS1-SA-2A-Puro-TLR targeting vector, a CAG-Venus+1-P2A+3-mtagRFP+3 cassette was cloned into SalI/NotI sites of AAVS1-SA-2A-Puro targeting vector (Addgene, #22075). In addition, a SA-2A-GFP fragment was generated by overlapping PCR and inserted into the XhoI/SalI sites of the AAVS1 targeting vector, with the GFP template derived from a pRosa26-IRES-GFP plasmid (V.T.C., unpublished). For reporter replacement in the mouse cell line, the P110*-IRES-BFP-pA construct was generated by overlapping PCR and cloned into the pSTblue-1 sequencing plasmid (Novagen). For PCR donor templates, fragments were amplified with Herculase II Fusion DNA Polymerase (Agilent Technology) from pVenus+1-P2A+3-tagRFP plasmid using the same forward primer and different reverse primers (**Supplementary Table 4**).

Generation of CRISPR-Cas9 vector expressing shRNA or Ad4 proteins. To generate CRISPR-Cas9-T2A-BFP/mCherry-hH1-shRNA vectors, we generated the human H1 promoter and MCS sequence by overlapping PCR and cloned it into the NotI site of the CRISPR-Cas9-T2A-BFP/mCherry plasmid. To obtain CRISPR-Cas9-T2A-BFP/mCherry-P2A-Ad E1B55K or E4orf6 plasmids, the coding regions for adenoviral serotype 4 proteins were synthesized as mammalian codon–optimized sequences (**Supplementary Table 1**) by Genscript (Piscataway, NJ, USA). Using these genes and BFP and mCherry template plasmids, we amplified BFP/mCherry-P2A-Ad4 E1B55K and BFP/mCherry-P2A-Ad4 E4orf6 fragments and cloned them into the NheI/EcoRI sites of the CRISPR-Cas9-T2A-reporter plasmid by Gibson assembly (New England Biolabs, E2611S).

sgRNA and shRNAs. sgRNAs were designed based on unique sequences with 20 nt and as the last nucleotide before the PAM signal an A or G was selected. The target sequences should hybridize with the sgRNA scaffold only at low energy as predicted by the Mfold web server (http://mfold.rna.albany.edu/?q=mfold/rna-folding-form). Complementary oligonucleotides were ordered separately, annealed, phosphorylated and cloned into the BbsI sites of the CRISPR-Cas9-T2A-reporter plasmid (**Supplementary Table 4**). For shRNA silencing, shRNA-targeted sequences were selected from previous reports[24–29] (**Supplementary Table 4**). Complementary oligonucleotides were ordered separately, annealed, phosphorylated and cloned into the BamHI/AflII sites of the CRISPR-Cas9-T2A-reporter-hH1 plasmid.

Transfection and electroporation. Human HEK293 and mouse NHI3T3 cells were plated into 24-well or 6-well plates at 1 day before transfection. On the day of transfection, these cells were supplied with new complete medium and the DNA mixed with FuGENE HD Reagent (Promega) in Opti-MEM (Invitrogen) according to the manufacturer's introduction. After 15 min of incubation at room temperature, the mixture was dropped slowly into the well. For electroporation, mouse BL cells were harvested and counted, $1–2 \times 10^6$ cells resuspended with 3 μg plasmid DNA in 100 ml electroporation buffer and transferred to a 0.2 cm cuvette (Sigma) and electroporated using a Nucleofactor device (Lonza). Then, cells were transferred into prewarmed complete medium.

Cell sorting and flow cytometry. For single-cell cloning, single cells were sorted into 96-well plates with 150 ml complete medium supplied with 10 μg/ml Gentamycin (Lonza). These plates were briefly centrifuged and incubated at 37 °C, 5% CO_2, the single-cell clones were evaluated 3 days after sorting to exclude multiple cell contamination. Cells were cultured until confluence and duplicated for genotyping PCR. For the bulk sorting, the reporter-positive cells were sorted into 15-ml Falcon tubes with complete medium, cells were centrifuged and further cultured or used for the isolation of genomic DNA. For flow cytometry analysis, HEK293 cells were trypsinized and resuspended in PBS/1% BSA FACS buffer and analyzed with a Fortessa machine (Becton Dickinson). Mouse BL cells were harvested, centrifuged and resuspended in PBS/1% BSA FACS buffer.

Genomic DNA isolation, PCR and T7EI assay. Reporter$^+$ cells were cultured and harvested at different time points. Single-cell clones were duplicated in 96-well plates. Genomic DNA was extracted using the QuickExtract DNA extraction kit (Epicentre) following the manufacturer's instruction. For T7EI assay, PCR was done using Herculase II Fusion DNA Polymerase (Agilent Technology) with PCR gene-specific primers (**Supplementary Table 4**) using the following conditions: 98 °C for 3 min; 35–37 cycles (95 °C for 20 s, 60 °C for 20 s, 72 °C for 20 s) and 72 °C for 3 min. PCR products were run on 2% agarose gels, purified, denatured, annealed and treated with T7EI (New England Biolabs). Cleaved DNA fragments were separated on 2% agarose gels and the DNA concentration of each band was quantified using the ImageJ software. Percent values of indels were calculated as described[30]. For genotyping PCR, genomic DNA was amplified using DreamTaq DNA Polymerase (Thermo Scientific) with primers listed in **Supplementary Table 4**.

DNA sequencing. PCR products were directly sequenced by specific primers or cloned into the pSTBlue-1 Blunt vector (Novagen) following the manufacturer's protocol. Plasmid DNAs were isolated using the NucleoSpin Plasmid (Macherey-Nagel). Plasmids were sequenced using T7 forward primer (`5′–TAATACGACTCACTATAGGG–3′`) by the Sanger method (LGCgenomics, Berlin, Germany).

Western blot analysis. Transfected AAVS1^{TLR} Reporter (BFP$^+$) cells were isolated by FACS and 10×10^6 cells were lysed on ice in RIPA buffer (20 mM Tris-HCl (pH 7.5), 150 mM NaCl 1, mM EDTA, 1% NP-40, 0.1% SDS, 0.1% sodium deoxycholate) for 20–30 min in the presence of protease inhibitors (Roche). The whole-cell lysates were centrifuged for 10 min at 14,000 r.p.m. The supernatants were transferred into new tubes and protein concentrations were determined using the BCA protein assay (Bio-Rad). The lysates were boiled at 100 °C for 5 min and loaded on SDS-PAGE gels. Blots were probed with anti-DNA ligase IV (H-300, Santa Cruz Biotechnology) and anti-beta-actin (AC-74, Sigma) antibodies. Blots were developed with secondary goat anti-rabbit IgG HRP (Southern Biotech) or anti-mouse IgG HRP (Southern Biotech) and bands visualized using the ECL detection kit (GE Healthcare).

22. Donnelly, M.L. *et al.* The 'cleavage' activities of foot-and-mouth disease virus 2A site-directed mutants and naturally occurring '2A-like' sequences. *J. Gen. Virol.* **82**, 1027–1041 (2001).
23. Merzlyak, E.M. *et al.* Bright monomeric red fluorescent protein with an extended fluorescence lifetime. *Nat. Methods* **4**, 555–557 (2007).
24. Martinez, J.J., Seveau, S., Veiga, E., Matsuyama, S. & Cossart, P. Ku70, a component of DNA-dependent protein kinase, is a mammalian receptor for Rickettsia conorii. *Cell* **123**, 1013–1023 (2005).

© 2015 Nature America, Inc. All rights reserved.

doi:10.1038/nbt.3198

25. Com, E. *et al.* Nerve growth factor receptor TrkA signaling in breast cancer cells involves Ku70 to prevent apoptosis. *Mol. Cell. Proteomics* **6**, 1842–1854 (2007).
26. Li, B., Reddy, S. & Comai, L. Depletion of Ku70/80 reduces the levels of extrachromosomal telomeric circles and inhibits proliferation of ALT cells. *Aging* **3**, 395–406 (2011).
27. Munakata, Y. *et al.* Ku80 autoantigen as a cellular coreceptor for human parvovirus B19 infection. *Blood* **106**, 3449–3456 (2005).
28. Muylaert, I. & Elias, P. Knockdown of DNA ligase IV/XRCC4 by RNA interference inhibits herpes simplex virus type I DNA replication. *J. Biol. Chem.* **282**, 10865–10872 (2007).
29. Windhofer, F., Wu, W. & Iliakis, G. Low levels of DNA ligases III and IV sufficient for effective NHEJ. *J. Cell. Physiol.* **213**, 475–483 (2007).
30. Cong, L. et al. Multiplex genome engineering using CRISPR-Cas systems. *Science* **339**, 819–823 (2013).

© 2015 Nature America, Inc. All rights reserved.

R.K. and W.W. are inventors on a patent application entitled "Improved recombination efficiency by inhibition of NHEJ DNA repair" (EP2718446).

© 2015 Nature America, Inc. All rights reserved.